Supporting Information

Damages induced by synchrotron radiation-based X-ray microanalysis in chrome yellow paints and related Cr compounds: assessment, quantification, and mitigation strategies

Letizia Monico,[1,2,3,] Marine Cotte,[4,5] Frederik Vanmeert,[3,6] Lucia Amidani,[4,7] Koen Janssens,[3,8] Gert Nuyts,[3] Jan Garrevoet,[9] Gerald Falkenberg,[9] Pieter Glatzel,[4] Aldo Romani,[1,2] Costanza Miliani[10]*

[1] CNR-SCITEC, via Elce di Sotto 8, 06123 Perugia, Italy

[2] SMAArt Centre and Department of Chemistry, Biology and Biotechnology, University of Perugia, via Elce di Sotto 8, 06123 Perugia, Italy

[3] AXES Research Group, NANOlab Centre of Excellence, University of Antwerp, Groenenborgerlaan 171, 2020 Antwerp, Belgium

[4] ESRF, Avenue des Martyrs 71, 38000 Grenoble, France

[5] LAMS, CNRS UMR 8220, Sorbonne Université, UPMC Univ Paris 06, Place Jussieu 4, 75005 Paris, France

[6] Laboratories of the Royal Institute of Cultural Heritage (KIK-IRPA), Parc du Cinquantenaire 1, 1000 Bruxelles, Belgium

[7] HZDR, Institute of Resource Ecology, Rossendorf Beamline at the ESRF, 01314 Dresden, Germany

[8] Rijksmuseum, Conservation & Restoration—Scientific Research, Hobbemastraat 22, 1071 ZC Amsterdam, The Netherlands

[9] DESY, Notkestraße 85, 22607 Hamburg, Germany

[10] CNR-ISPC, via Cardinale Guglielmo Sanfelice 8, 80134 Napoli, Italy

**email: letizia.monico@cnr.it*

Table of Contents

S1. Cr oxidation state mapping and linear combination fitting (LCF) of Cr K-edge XANES spectra

Cr oxidation state maps were obtained by setting the energy of the incoming X-ray beam at two energies: (i) at 5.993 keV, for favoring the excitation of Cr^{VI}-species, and (ii) at 6.090 keV for collecting XRF signals of all Cr species. The procedure used to extract the Cr oxidation state maps is described elsewhere.[1]

XANES spectra in XRF mode were recorded by scanning the primary energy in the 5.98-6.107 keV range with energy increments of 0.2 eV (total number of energy points: 650; exposure time: 0.1 s/point). The LCF of the spectra against a library of XANES profiles of Cr reference powders allowed the relative amount percentage of Cr^{VI}- and Cr^{III}-species [expressed as $[Cr^{VI}]/[Cr_{total}]$ (%) and $[Cr^{III}]/[Cr_{total}]$ (%), respectively] as a function of the fluence and absorbed dose to be determined.

As earlier described,[1,2,3,4,5] two or three components, namely one Cr^{VI}-compound ($PbCrO_4$/$PbCr_{0.2}S_{0.8}O_4$) plus Cr^{III}-oxides [$Cr(OH)_3$/Cr_2O_3] and/or either Cr^{III}-acetate hydroxide or Cr^{III}-acetylacetonate were required to obtain a good description of the XANES spectra (see Figure 4 and Figures S4, S6 for a selection of the results).

S2. Calculation of the absorbed dose

At a specific energy and fluence value, the absorbed dose of each analysis was calculated according to the following equation:

$$\text{Abs. dose (MGy)} = \text{fluence } (\text{ph} \cdot \mu\text{m}^{-2}) \times \text{mass att. coef. } (\text{cm}^2 \cdot \text{g}^{-1}) \times \text{energy/ph } (\text{J} \cdot \text{ph}^{-1}) \times 10^5$$

For each material, the mass attenuation coefficient was estimated using the tool available in the software PyMca,[6] that required as input values the density of the material (g cm^{-3}) and its mass fraction. As an example, the total mass attenuation coefficient of $PbCrO_4$ *vs.* the energy of the incident X-ray beam is reported in Figure S1.

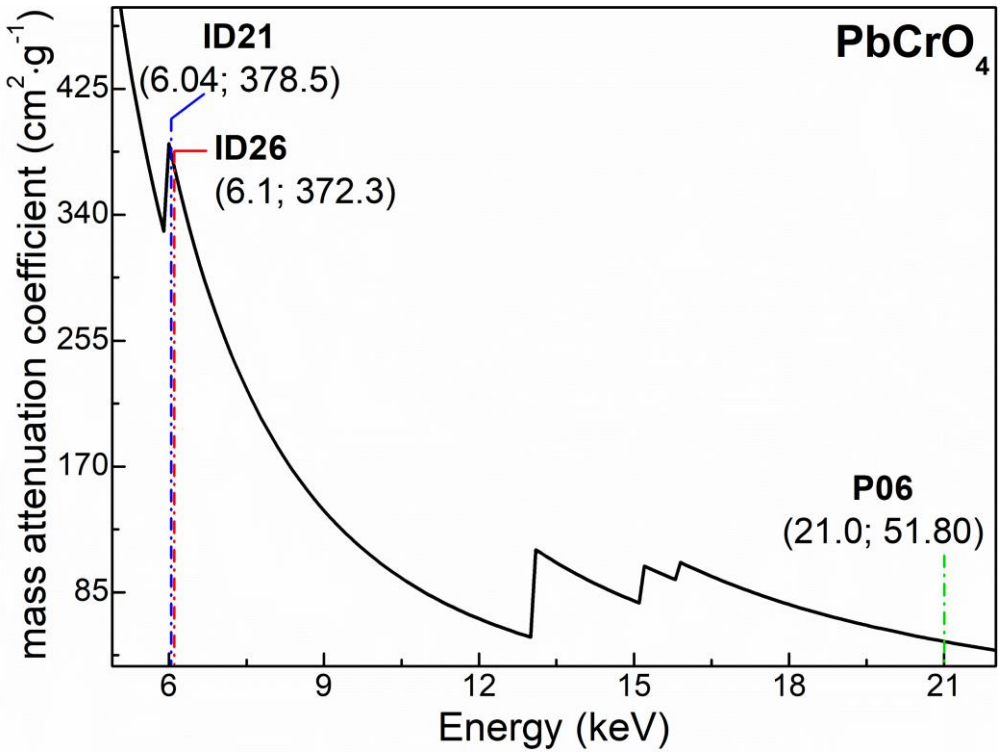

Figure S1. Total mass attenuation coefficient of $PbCrO_4$ *vs.* energy of the incident X-ray beam calculated using the software PyMca. The attenuation coefficient values extrapolated at the three beamlines where experiments were performed are also reported.

For chrome yellow mock-ups, the mass attenuation coefficient, and thus the absorbed dose, are lower when taking into account also the contribution of the binder (ca. 20% in our case). Nevertheless, in real paintings the exact pigment:binder ratio is not known. Thus, to better facilitate the comparison between the results of this work and those related to studies on original paint samples, we decided to not take into account the presence of the binder.

S3. Determination of the photon flux at beamline ESRF-ID26

At beamline ESRF-ID26, without using slits, the size of the beam was 0.6×0.075 mm^2 (h×v) and the photon flux was ~5×10^{12} ph·s^{-1}.

In the presence of slits, the photon flux could be considered the same in the vertical direction of the beam (slits at 0.15 mm), while it depends on the size of the employed slits in the horizontal direction. The photon flux using slits at either 0.5 mm or 0.7 mm, was obtained by calculating the integrals of a Gaussian curve which have a full width at half maximum (FWHM) of 0.6 mm (i.e., beam size in the horizontal direction) and an area of 5×10^{12} ph·s^{-1} (i.e. photon flux value in the absence of slits). The calculation, performed in the -0.250-0.250 mm range (slits at 0.5 mm) and in the -0.350-0.350 mm range (slits at 0.7 mm) around the maximum of the Gaussian curve, gives rise to values of about 3.37×10^{12} ph·s^{-1} and 4.15 ×10^{12} ph·s^{-1}, respectively. It follows that the employed slits have produced an attenuation of the original photon flux from *ca.* 20% to 30%.

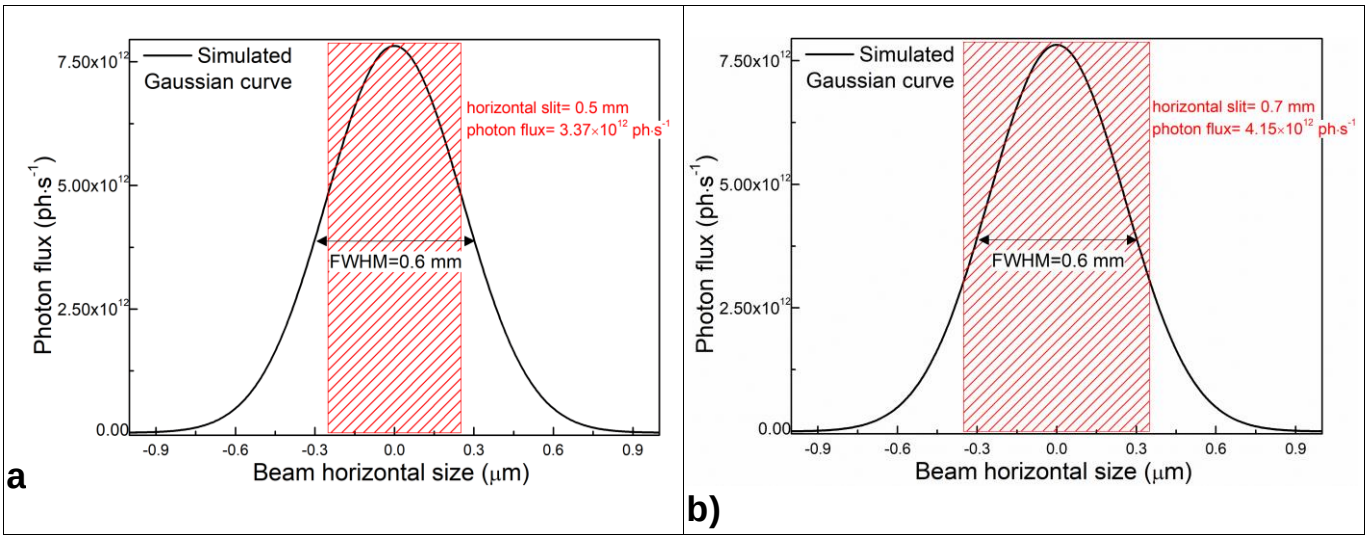

Figure S2. Calculation of the photon flux for the ESRF-ID26 experiment by considering the different size of horizontal slits: a) slits at 0.5 mm; b) slits at 0.7 mm. Values were obtained by calculating the integrals of a Gaussian curve (FWHM=0.6 mm; Area=5×10^{12} ph·s^{-1}), which was simulated using the software Origin 8.1.

In the case of the most X-ray sensitive samples, the photon flux was further decreasing to about 1×10^{10} ph·s^{-1} by employing attenuators.

S4. Cr-Kβ XES spectra: Kβ main lines

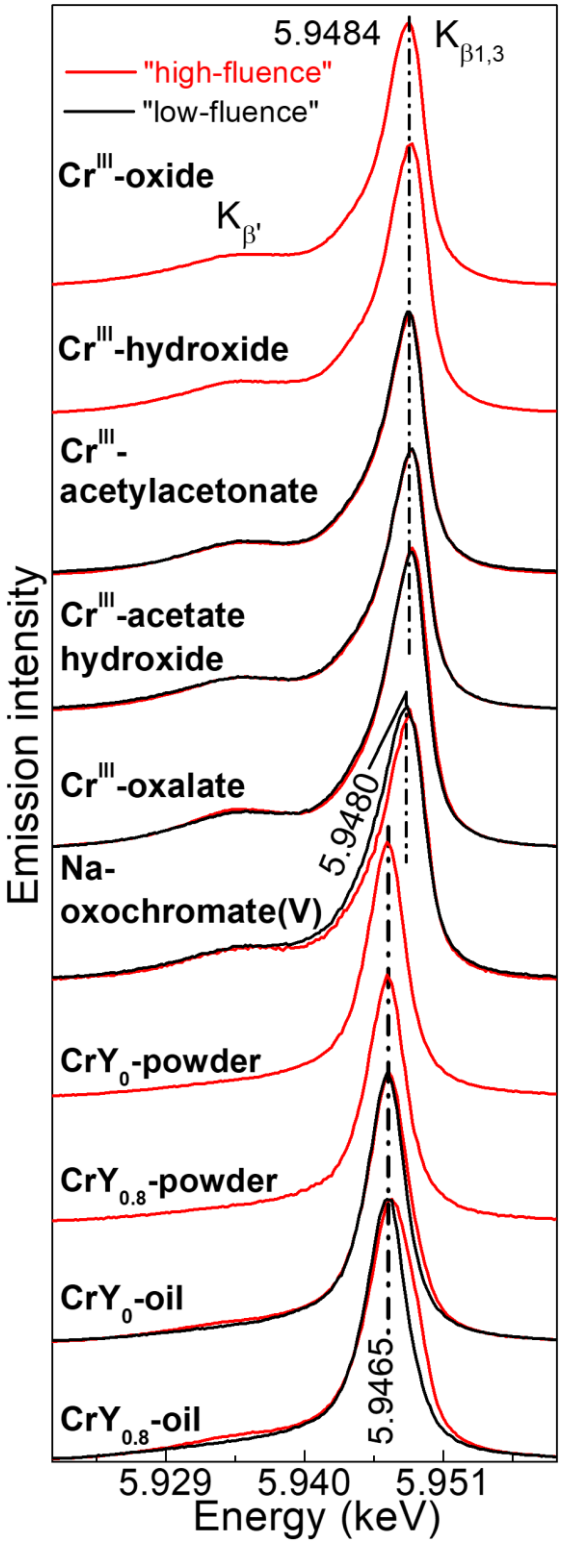

Figure S3. Kβ main lines region of the Cr-Kβ XES spectra recorded from Cr samples at "high-fluence" (red) and "low-fluence" (black) conditions (*cf.* Figure 2). Data were recorded at ESRF-ID26.

S5. LCF results of a selection of the Cr K-edge μ-XANES spectra recorded at room temperature and at variable fluences

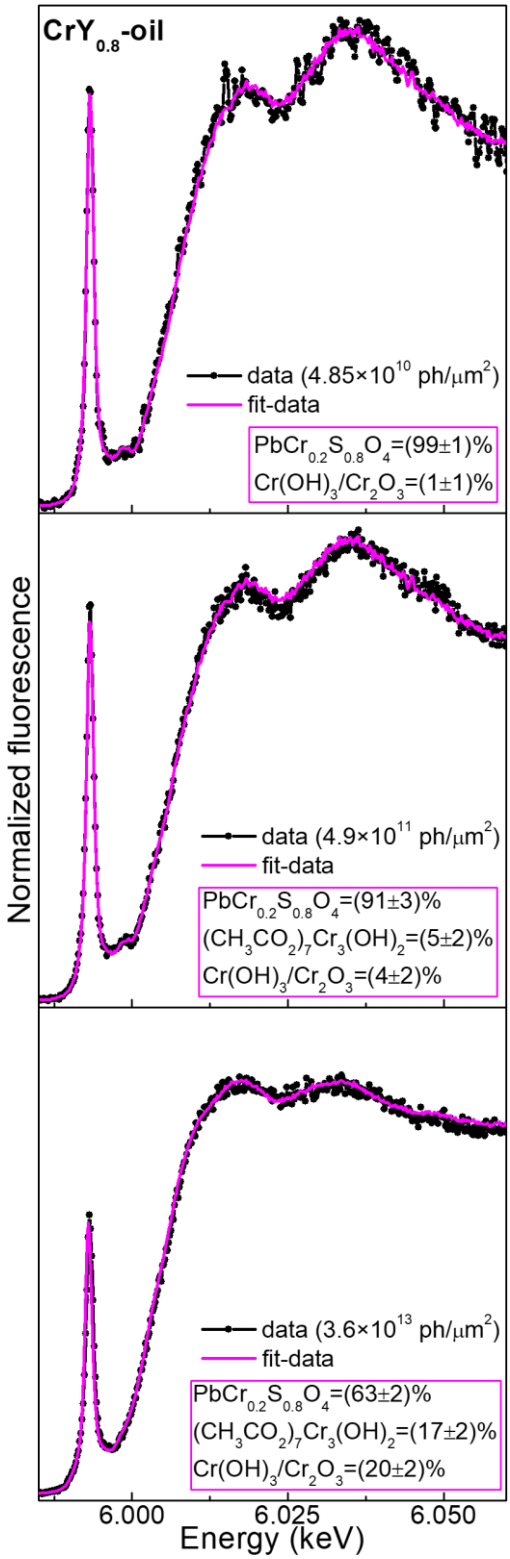

Figure S4. LCF results (magenta) of selected Cr K-edge XANES spectra (black) recorded from $CrY_{0.8}$-oil at room temperature and at different fluences (*cf.* Figure 3a for the complete set of results). Data were acquired at ESRF-ID21.

S6. Vibrational micro-spectroscopy measurements of chrome yellow oil paints "burnt" by "high-fluence" Cr-K_β XES investigations

Micro-FT-IR. Reflection mode measurements were carried out using a JASCO IMV-4000 interfaced with a FTIR 4100 spectrometer. Spectra were acquired from size areas of 312×312 μm^2 (Cassegrain 32x objective) in the 6000-600 cm^{-1} range, at 4 cm^{-1} resolution and using 4000 scans.

Micro-Raman. Analysis were performed by means of a JASCO NRS-3100 double-grating spectrophotometer equipped with a charge coupled device (CCD) detector cooled down to -47 °C and to an optical microscope (100x objective). Spectra were collected using a 488.0 nm excitation wavelength (Argon ion laser). The laser power at the sample was kept around 1 mW and a 1200 lines/mm^{-1} grating was employed. Spectra were recorded in the energy range of 2340-80 cm^{-1}, with 10 s exposure time and 7 accumulations.

Micro-FT-IR analysis performed in the "burnt" areas of sample $CY_{0.8}$-oil sample (Figure S5a: black line) reveal that "high-fluence" Cr-K_β XES investigations have induced the alteration of the oil, as shown by the disappearing of the characteristic IR bands positioned in the 3000-2800 cm^{-1} range and at *ca.* 1735 cm^{-1}. Minor changes appear also in the sulfate asymmetric stretching mode (1230-920 cm^{-1}) of the pigment.

In addition, micro-Raman measurements (Figure S5b) reveal the presence of carbon black. Overall, the results show that, next to the degradation of the chrome yellow pigment, also a significant alteration of the binder took place.

Comparable results have been obtained for CY_0-oil paint. Thus, they are not reported in Figure S5.

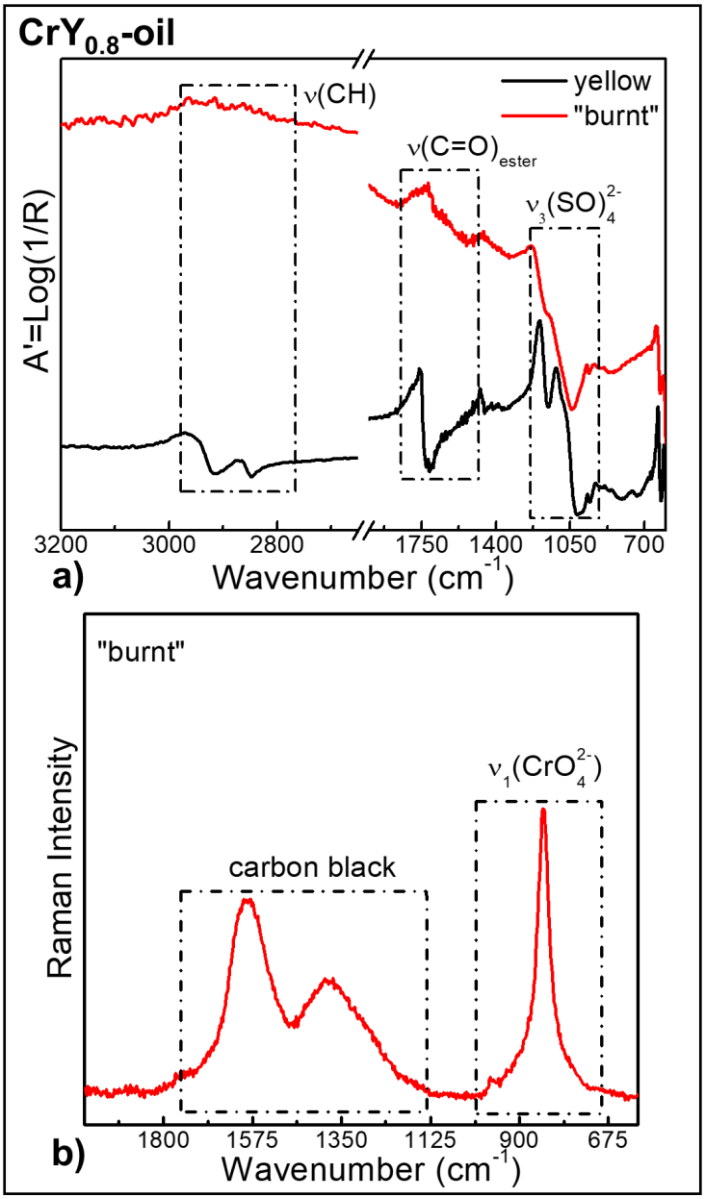

Figure S5. (a) Reflectance micro-FT-IR and **(b)** micro-Raman spectra recorded from $CrY_{0.8}$-oil paint: (black) unexposed yellow area and (red) "burnt" areas where "high-fluence" Cr-K_β XES investigations have performed (*cf.* Figure 4b).

S7. Cr oxidation state mapping and Cr K-edge μ-XANES analysis of the areas "burnt" by μ-XRD damage experiments

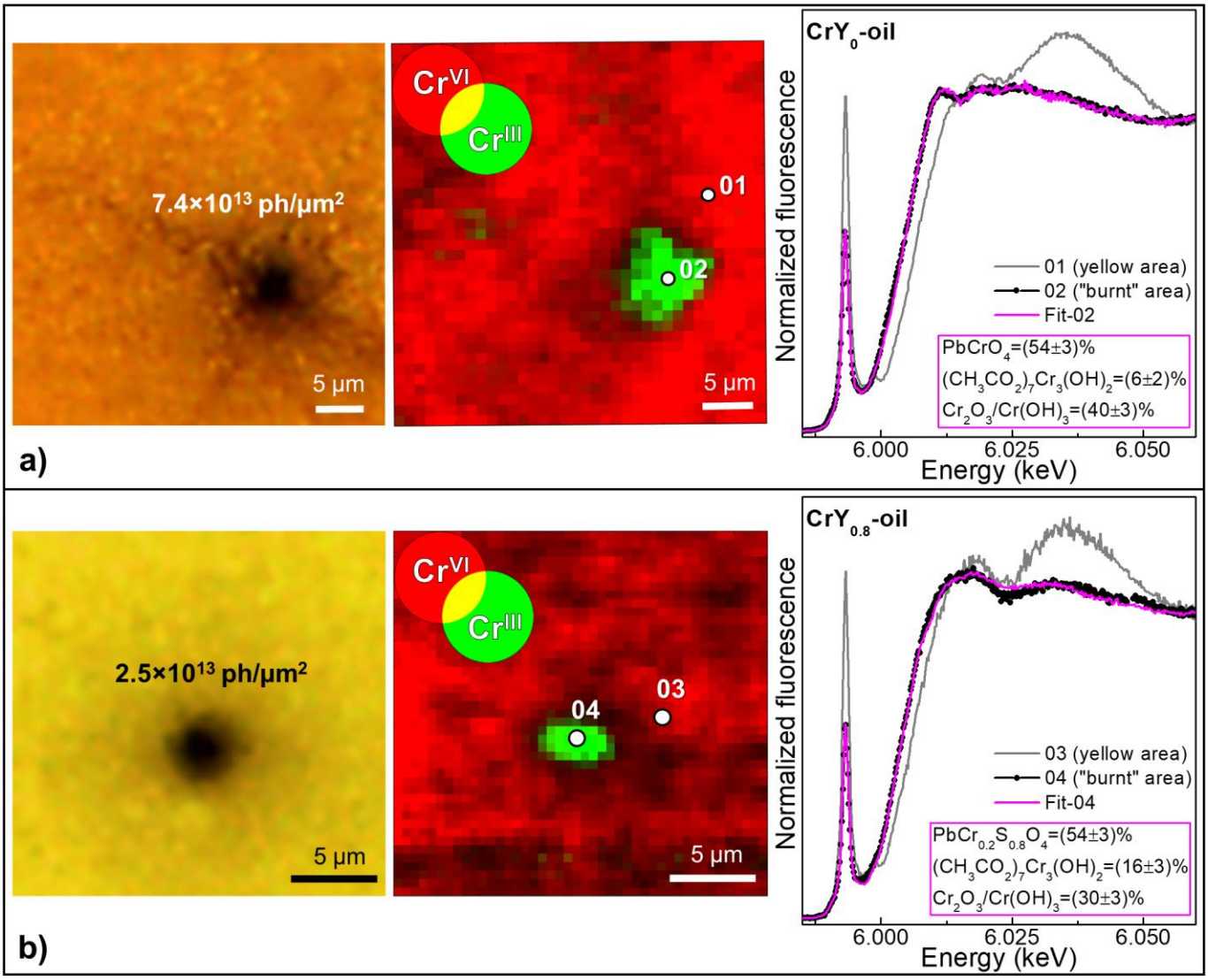

Figure S6. Cr speciation results obtained at ESRF-ID21 from **(a)** CrY_0-oil and **(b)** $CrY_{0.8}$-oil paints after X-ray-induced damage tests performed at DESY-P06: (from left) photomicrographs showing the "burnt" areas induced by fluences of **(a)** 7.4×10^{13} ph/μm² and **(b)** 2.5×10^{13} ph/μm² (*cf.* Figure 5 for the corresponding μ-XRD results), RG composite SR μ-XRF Cr^{VI}/Cr^{III} maps [step size (h×v): down to 0.5×0.5 μm²; exp. time: 100 ms/pixel] and Cr K-edge XANES spectra recorded from the yellow area (grey) and "burnt" spots (black) with corresponding LCF results (magenta).

S8. Relationship between the X-ray photo-induced reduction of Cr^{III} and fluence rate

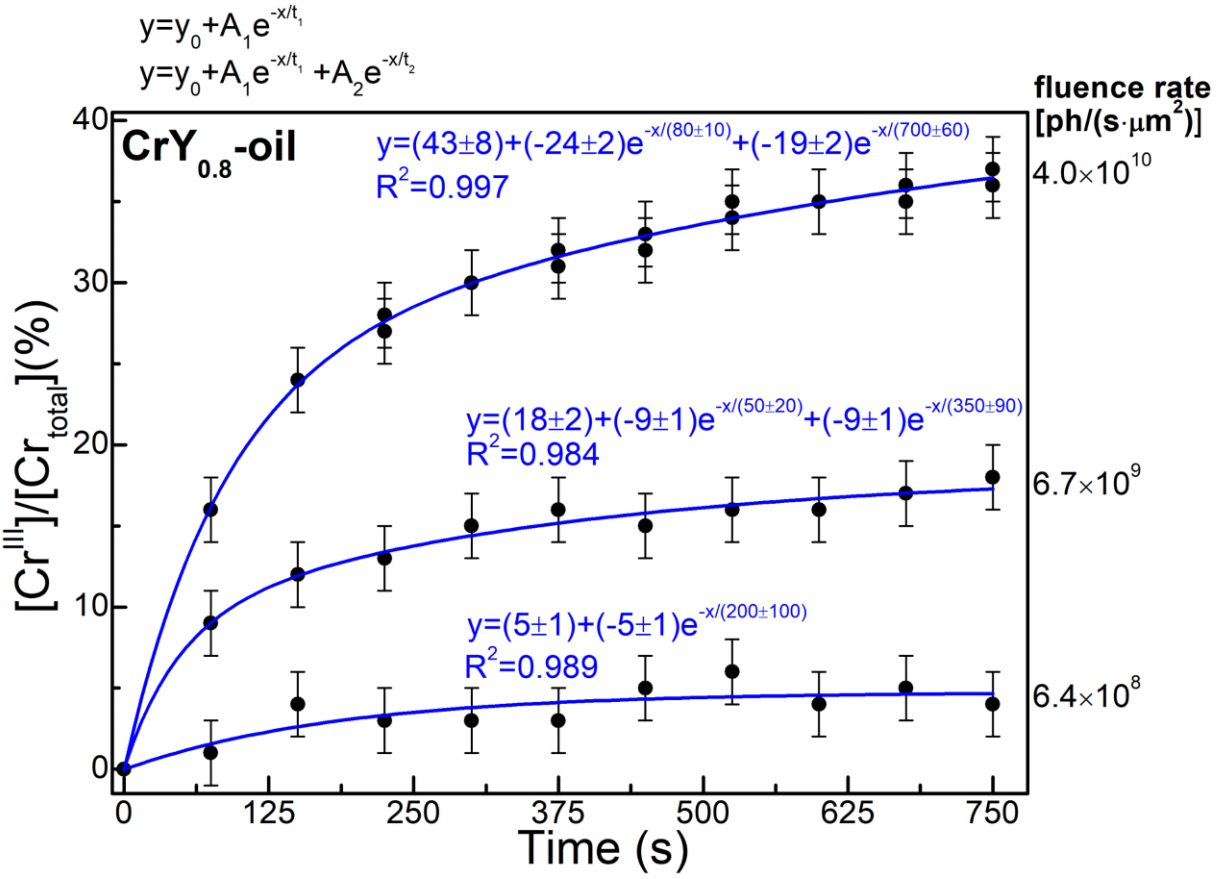

Figure S7. Plots of Cr^{III}-relative amount percentage *vs.* time obtained from $CrY_{0.8}$-oil paint at different fluence rates and room temperature (see Figure 3a for the equivalent data reported as a function of the fluence/absorbed doses). In blue, fit obtained by employing mono-exponential and bi-exponential functions. Data were collected at ESRF-ID21. The highest fluence rate value was obtained without attenuation of the incoming X-ray beam, while the others two using Al attenuators of different thickness (20 µm and 100 µm).

References

[1] Monico, L.; Van der Snickt, G.; Janssens, K.; De Nolf, W.; Miliani, C.; Verbeeck, J.; Tian, H.; Tan, H.; Dik, J.; Radepont, M.; Cotte, M. Degradation Process of Lead Chromate in Paintings by Vincent van Gogh Studied by Means of Synchrotron X-ray Spectromicroscopy and Related Methods. 1. Artificially Aged Model Samples. *Anal. Chem.* **2011***, 83*, 1214-1223.

[2] Monico, L.; Janssens, K.; Miliani, C.; Van der Snickt, G.; Brunetti, B. G.; Cestelli Guidi, M.; Radepont, M.; Cotte, M. Degradation Process of Lead Chromate in Paintings by Vincent van Gogh Studied by Means of Spectromicroscopic Methods. 4. Artificial Aging of Model Samples of Co-Precipitates of Lead Chromate and Lead Sulfate. *Anal. Chem.* **2013**, *85,* 860-867.

[3] Monico, L.; Janssens, K.; Cotte, M.; Romani, A.; Sorace, L.; Grazia, C.; Brunetti, B. G.; Miliani, C. Synchrotron-based X-ray spectromicroscopy and electron paramagnetic resonance spectroscopy to investigate the redox properties of lead chromate pigments under the effect of visible light. *J. Anal. At. Spectrom.* **2015***, 30,* 1500-1510.

[4] Monico, L.; Janssens, K.; Cotte, M.; Sorace, L.; Vanmeert, F.; Brunetti, B. G.; Miliani, C. Chromium speciation methods and infrared spectroscopy for studying the chemical reactivity of lead chromate-based pigments in oil medium. *Microchem. J.* **2016**, *124*, 272-282.

[5] Monico, L.; Sorace, L.; Cotte, M.; De Nolf, W.; Janssens, K.; Romani, A.; Miliani, C. Disclosing the Binding Medium Effects and the Pigment Solubility in the (Photo)reduction Process of Chrome Yellows ($PbCrO_4$/$PbCr_{1-x}S_xO_4$). *ACS Omega* **2019***, 4,* 6607-6619.

[6] Cotte, M.; Fabris, T.; Agostini, G.; Motta Meira, D.; De Viguerie, L.; Solé, V.A. . Watching kinetic studies as chemical maps using open-source software. *Anal. Chem.* **2016***, 88,* 6154-6160.